Probing Anomalous Relaxation by Coherent Multidimensional Optical Spectroscopy

František Šanda[1,*] and Shaul Mukamel[2,†]

[1]Charles University, Faculty of Mathematics and Physics, Ke Karlovu 5, Prague, 121 16 Czech Republic
[2]Department of Chemistry, University of California, Irvine, California 92697-2025, USA

(Received 9 September 2006; published 22 February 2007)

We propose to study the origin of algebraic decay of two-point correlation functions observed in glasses, proteins, and quantum dots by their nonlinear response to sequences of ultrafast laser pulses. Power-law spectral singularities and temporal relaxation in two-dimensional correlation spectroscopy signals are predicted for a continuous time random walk model of stochastic spectral jumps in a two-level system with a power-law distribution of waiting times $\psi(t) \sim t^{-\alpha-1}$. Spectroscopic signatures of stationary ensembles for $1 < \alpha < 2$ and aging effects in nonstationary ensembles with $0 < \alpha < 1$ are identified.

DOI: 10.1103/PhysRevLett.98.080603 PACS numbers: 05.40.Fb, 02.50.−r, 42.65.−k, 78.47.+p

Exponential relaxation profiles and correlation functions observed in systems coupled to a bath with a short correlation time are signatures of fast memory loss. Such normal relaxation can be described by Markovian (e.g., Langevin, Fokker-Planck, and master) equations of motion; multipoint Green's functions may then be factorized into products of two-point functions and carry no additional information. However, correlation functions in many systems characterized by a complex free-energy landscape with a broad distribution of dynamical barriers [1] may acquire long stretched-exponential or algebraic tails [2]. Anomalous variations of fluorescence emission (blinking) has been observed in biomolecules [3], polymers [4], quantum dots [5–7], and glasses. The fluorescence trajectories are commonly analyzed using a continuous time random walk (CTRW) model of spectral diffusion. In this Letter, we demonstrate how spectral line shapes obtained from two-dimensional correlation spectroscopy (2DCS) [8] may be used to probe complex anomalous relaxation processes in the condensed phase. 2DCS techniques are femtosecond optical analogues of NMR, that have been successfully employed towards the study of the structure of peptides [9], chemical exchange in liquids [10], and exciton migration in photosynthetic antennae [11]. 2DCS provides a bulk alternative to single molecule measurements of multipoint correlation functions [3] that is useful for testing microscopic dynamic model. Connection to anomalous relaxation requires a consistent theory of 2DCS signals with non-Markovian spectral fluctuations, which is the goal of this Letter.

The CTRW model is defined by a waiting time probability density function (WTDF) $\psi(t)$ for stochastic jumps between various states. All memory is erased at the time of the jump. This renewal (resetting) property makes it possible to compute all statistical measures even in the absence of a Markovian description for the probability distribution, and provides a convenient formalism for describing long-term memory effects. When $\psi(t)$ has an exponential form $\psi(t) = \exp(-t/\kappa_1)$ (where $\kappa_1 \equiv \int_0^\infty t\psi(t)dt$ is mean waiting time), the system may also be described by a Markovian master equation, and the relaxation is normal. However, models with a long-time algebraic decay $\psi(t) \sim t^{-\alpha-1}$ show anomalous phenomena at long times when the second moment of $\psi(t)$ diverges $0 < \alpha < 2$.

We consider a random walk which is observed starting at time 0. The WTDF of the first jump $\psi'(t)$ may differ from $\psi(t)$ since it depends on how the system was prepared before $t = 0$. It must be treated with care since it strongly affects the nature of the anomalous ensemble. Stationary processes must satisfy microscopic reversibility, which implies that $\psi'(t)$ is given by a product of the survival probability $\phi(t) = \int_t^\infty \psi(t')dt'$ that no jump had occurred for time t and the equilibrium density of jumps $1/\kappa_1$, resulting in $\psi'(t) = \phi(t)/\kappa_1$ [12]. A stationary CTRW is thus only possible for $1 < \alpha < 2$ where the first moment κ_1 is finite. The resulting power-law relaxation is slow, but eventually the system reaches an equilibrium [13]. For $0 < \alpha < 1$, κ_1 diverges. The system never equilibrates and shows aging effects (i.e., dependence on the initial observation time). Aging phenomena are commonly studied by preparing a nonstationary ensemble where all particles are assumed to make a jump at the time origin, so that $\psi'(t) = \psi(t)$. Signatures of aging were observed in fluorescence blinking of single CdSe quantum dots, analyzed within CTRW, and yielded $\alpha \approx 0.5$ [6,7,14]. In contrast, the anomalous multipoint correlations observed in fluorescence trace of conformation dynamics of flavin proteins [3] showed symmetries due to microscopic reversibility indicative of a stationary process.

We consider a system undergoing anomalous stochastic jumps between two states a and b. The system is further coupled to a two-level chromophore with a ground $|g\rangle$ and an excited state $|e\rangle$ and dipole moment μ_{eg}, causing its transition frequency Ω_{eg} to undergo stochastic fluctuations $\delta\Omega_{eg}(t)$. $\delta\Omega_{eg}$ can assume two values Ω_0 and $-\Omega_0$ corresponding to the system being in state a and b, respec-

tively. This is known as the two state jump (TSJ) model of spectral line shapes [15]. Observable quantities are obtained by averaging over the ensemble of stochastic paths of $\delta\Omega_{eg}(t)$.

We propose to probe this complex dynamics through the four-wave-mixing signal generated by the coherent response of the chromophore to three short optical pulses with wave vectors $\mathbf{k_1}$, $\mathbf{k_2}$, and $\mathbf{k_3}$ at times 0, t_1, $t_1 + t_2$. The signal detected at time $t_1 + t_2 + t_3$ is described by the nonlinear response function which depends on the three experimentally controlled parameters t_1, t_2, t_3. The photon echo signal generated in the $\mathbf{k_I} = -\mathbf{k_1} + \mathbf{k_2} + \mathbf{k_3}$ phase-matching direction is given by [16]

$$\mathcal{S}_{\mathrm{I}}(t_1, t_2, t_3) = 2(i/\hbar)^3 \mu_{eg}^4 \theta(t_3)\theta(t_2)\theta(t_1) e^{i\Omega_{eg}(\eta t_1 - t_3)} e^{-\Gamma(t_1+t_3)} \left\langle \exp\left[-i\int_{t_1+t_2}^{t_1+t_2+t_3} \delta\Omega_{eg}(\tau)d\tau\right] \exp\left[i\eta\int_0^{t_1} \delta\Omega_{eg}(\tau)d\tau\right]\right\rangle, \tag{1}$$

with $\eta = 1$. We have added a homogenous dephasing rate Γ. We shall display this signal by 2D ω_1, ω_3 correlation plots

$$\mathrm{S}_{\mathrm{I}}(\omega_1, t_2, \omega_3) = -\mathrm{Im}\iint \mathcal{S}_{\mathrm{I}}(t_1, t_2, t_3) e^{i(\omega_1 t_1 + \omega_3 t_3)} dt_1 dt_3, \tag{2}$$

where t_2 is held fixed. A different signal, $\mathcal{S}_{\mathrm{II}}$, generated in the $\mathbf{k_{II}} = \mathbf{k_1} - \mathbf{k_2} + \mathbf{k_3}$ direction is similarly given by setting $\eta = -1$. We further display the combination $\mathrm{S}_A(\omega_1, t_2, \omega_3) \equiv \mathrm{S}_{\mathrm{I}}(-\omega_1, t_2, \omega_3) + \mathrm{S}_{\mathrm{II}}(\omega_1, t_2, \omega_3)$ which shows absorptive peaks [17]. An optical coherence is encoded in the system during t_1 and probed during t_3. By varying the delay t_2 between these periods (which is typically much longer than t_1 and t_3), we can explore correlations between dynamical events of the stochastic system. Multipoint correlation functions ordinarily obtained in single molecule spectroscopy can thus be obtained from bulk measurements.

Microscopic reversibility in stationary ensembles implies that $\mathcal{S}_{\mathrm{I}}(t_3, t_2, t_1) = -\mathcal{S}_{\mathrm{I}}^*(t_1, t_2, t_3)$ and $\mathcal{S}_{\mathrm{II}}(t_3, t_2, t_1) = \mathcal{S}_{\mathrm{II}}(t_1, t_2, t_3)$, resulting in the following symmetry of the line shape

$$\mathrm{S}_A(\omega_3, t_2, \omega_1) = \mathrm{S}_A(\omega_1, t_2, \omega_3). \tag{3}$$

When the system has no memory during the t_3 interval regarding its state during t_1, $\mathcal{S}_{\mathrm{I}}$ and $\mathcal{S}_{\mathrm{II}}$ may be factorized as $\mathcal{S}_{\mathrm{I}}(t_1, t_2, t_3) = 2(i/\hbar)K(t_3)K^*(t_1)$ and $\mathcal{S}_{\mathrm{II}}(t_1, t_2, t_3) = 2(i/\hbar)K(t_3)K(t_1)$. Here, $K(t) \equiv (i/\hbar)\mu_{eg}^2 e^{-(\Gamma + i\Omega_{eg})t}\langle\exp[-i\int_0^t \delta\Omega_{eg}(\tau)d\tau]\rangle$ is the linear response function. The correlation signal reduces in this case to the product of the linear absorption $W_A(\omega) \equiv \mathrm{Im}\int_0^\infty K(t)\exp[i\omega t]dt$ line shapes

$$\hbar\,\mathrm{S}_A(\omega_1, t_2 \to \infty, \omega_3) = 4W_A(\omega_1)W_A(\omega_3). \tag{4}$$

Algebraic memory will result in a slow convergence to this asymptotic line shape. In addition, the spectra will diverge at certain frequencies where the factorization [Eq. (4)] does not hold, as will be shown below.

The response functions will be calculated by introducing a 2×2 matrix $\hat{G}_\nu$ in a, b space whose jl element gives the contribution of paths with initial state l and final state j by averaging over l and summing over j.

$$\mathcal{S}_\nu(t_1, t_2, t_3) = \sum_{jl} (G_\nu)_{jl}(t_1, t_2, t_3)[\rho]_l(t = 0) \tag{5}$$

In the case of Markovian relaxation, G_ν is given by a product of three Green's functions representing the time evolution during the t_1, t_2, and t_3 intervals. These Green's functions can be calculated by solving the stochastic Liouville equation, which combines the Liouville equation for coherence evolution with a rate equation for the jumps [18]. The anomalous four-point $\hat{G}_\nu$, in contrast, may not be factorized in this manner. Calculating it requires some bookkeeping of jump events. For each of the three time intervals t_1, t_2, t_3, we distinguish between two possibilities: either there was no jump or there was at least one jump during that interval. According to this classification, $\hat{G}_\nu$ is given by a sum of 8 terms $\hat{G}_\nu^m$, $(m = 1, \ldots, 8)$. $\hat{G}_\nu^m$ are constructed by convoluting matrix factors for propagation between the first and the last jump in the t_i interval (if any jump occurred in t_i) and factors for the coherent evolution between the consecutive jumps in different intervals (last in earlier and first in later) [12]. The calculation is conveniently made in Laplace domain where convolutions become simple multiplications and the integral equation for the propagator factor becomes an algebraic equation. Making use of the causality of the response functions [Eq. (1)], the 2D line shapes [Eq. (2)] were obtained by analytical continuation of the Laplace domain response functions calculated in Appendix D of Ref. [12] by setting $s_1 = \Gamma + i\eta(\omega_1 - \Omega_{eg})$, and $s_3 = \Gamma - i(\omega_3 - \Omega_{eg})$, where s_j is the Laplace variable conjugated to t_j.

We first consider a stationary ensemble with anomalous relaxation where [12]

$$\tilde{\psi}_W(s) = \frac{1}{1 + \kappa_1 s/[1 + (\kappa_\alpha s)^{\alpha-1}]}; \qquad 1 < \alpha < 2; \tag{6}$$

$\tilde{\psi}(s)$ is the Laplace transform of $\psi(t)$. This WTDF has a mean waiting time κ_1 and the long-time $t \gg (\kappa_1\kappa_\alpha^{\alpha-1})^{1/\alpha}$ asymptotics $\psi_W(t) \sim \kappa_\alpha^{\alpha-1}\kappa_1/t^{\alpha+1}$. In all plots, we use the dimensionless frequency units $(\omega_j - \Omega_{eg})/\Omega_0$ by setting $\Omega_{eg} = 0$, $\Omega_0 = 1$.

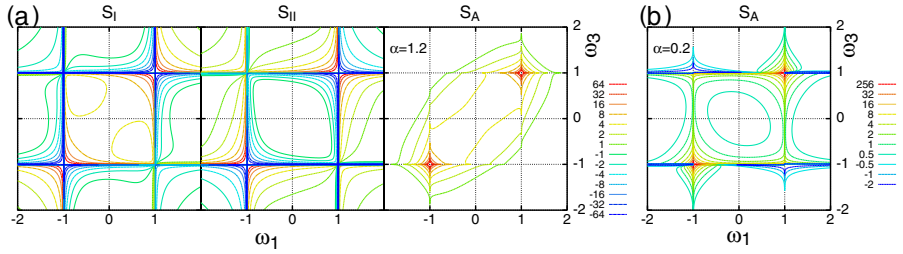

FIG. 1 (color online). (a): The 2D $S_{\rm I}(-\omega_1, \omega_3)$ (left), $S_{\rm II}(\omega_1, \omega_3)$ (middle), and $S_A(\omega_1, \omega_3)$ (right) signal [Eq. (1)] for the WTDF [Eq. (6)] at $t_2 = 0$, for $\alpha = 1.2$, and $\kappa_\alpha/\kappa_1 = 0.25, \Omega_0\kappa_1 = 2.0, \Omega_0 = 1, \Omega_{eg} = 0$. (b): The 2D S_A signal for the nonstationary random walk $\alpha = 0.2$, $t_2 = 0$, $t_{in} = 0$ $\kappa\Omega_0 = 2.0$, $\Omega_0 = 1$, $\Omega_{eg} = 0$.

No jumps occur during t_1 and t_3 in the slow fluctuation $\Omega_0\kappa_1 \gg 1$ limit. The linear line shape has two peaks at frequencies $\omega = \pm 1$, and the 2D spectrum for short delay $t_2 \sim 0$ consists of two diagonal peaks (the system is in the same state during t_1 and t_3) at (ω_1, ω_3), (1,1), and $(-1, -1)$. For normal relaxation, the peaks are Lorentzian. The anomalous model shows the same peak pattern, but the peaks are divergent due to long-tailed correlations. For $\Gamma = 0$, the linear absorption peaks diverge as $\Delta\omega^{\alpha-2}$ where $\Delta\omega_1 \equiv \omega_1 - \Omega_{eg} - \Omega_0$ [12,15].

In Fig. 1(a), we display the $S_{\rm I}$, $S_{\rm II}$, and S_A signals for slow fluctuations at $t_2 = 0$ and $\Gamma = 0$. All panels show prominent two diagonal peaks at (1, 1) and $(-1, -1)$. S_A is simpler due to interference of $S_{\rm I}$ and $S_{\rm II}$, which have opposite signs in specific $\Delta\omega_1$, $\Delta\omega_3$ quadrants, and substantially cancel. Along the $\omega_1 = \pm 1$ and $\omega_3 = \pm 1$ lines, $S_{\rm I}$ and $S_{\rm II}$ diverge as $\sim\Delta\omega_3^{\alpha-2}$ and $\sim\Delta\omega_1^{\alpha-2}$, respectively. S_A is finite along $\omega_1 = \pm 1$ (except for the $\omega_3 = \pm 1$ peaks), but is nondifferentiable with respect to ω_1. The $\omega_3 = \pm 1$ line has the same analytical structure.

The most rapidly divergent term $\hat{G}^8_\nu$, which represents the paths that have no jump during the entire time $t_1 + t_2 + t_3$, is given by (for the (1,1) diagonal peak)

$$S^{\,8}_A(\omega_1, t_2 = 0, \omega_3) = \frac{2\mu_{eg}^4}{\hbar^3}\left[\frac{\Delta\omega_3}{\Delta\omega_3^2 - \Delta\omega_1^2}\,\mathrm{Im}\tilde{\phi}'(\Gamma - i\Delta\omega_3) + \frac{\Delta\omega_1}{\Delta\omega_1^2 - \Delta\omega_3^2}\,\mathrm{Im}\tilde{\phi}'(\Gamma - i\Delta\omega_1)\right]. \quad (7)$$

For $\Gamma > 0$, Eq. (7) is regular; for $\Gamma = 0$, it diverges as $S_A \approx \frac{2\mu_{eg}^4}{\hbar^3}\kappa_\alpha^{\alpha-1}\sin[\pi(2-\alpha)/2]\Delta\omega_3^{\alpha-3}$ $(\Delta\omega_3 \to 0,\ \Delta\omega_1 = 0)$. This is illustrated in the linear log-log plot in Fig. 2(a) showing in S_A vs ω_3 for $\omega_1 = 1$. The $\alpha - 3$ exponent is shown in the inset.

For fast fluctuations $\Omega_0\kappa_1 \ll 1$ (not shown), the state of the system rapidly changes during the t_1, t_3 intervals. For normal relaxation, both 1D and 2D line shapes then consist of a single Lorentzian at the average frequency (motional narrowing). For anomalous dynamics, the survival probability in the initial state is substantial even for fast fluctuations, and the two peak divergencies of the slow limit (Fig. 1(a)) are still retained. An additional central peak at (0,0) shows up.

The variation of S_A with delay time t_2 in the slow fluctuation limit is displayed in Fig. 3. We see a buildup of (finite, as shown at the right panel) off-diagonal cross-peaks, whose line shapes are dominated by paths where the system is in a different state during t_1 and t_3. The $(-1, 1)$ peak represents paths where the system was in state b during t_1 and a during t_3. The $(1, -1)$ peak represents the reverse sequence. Note that this 2DCS equilibrium measurement records subensembles of trajectories without having to perturb the system or perform a single molecule measurement. Contour elongation of both diagonal and cross peaks along the $\omega_{1,3} = \pm 1$ directions is a signature

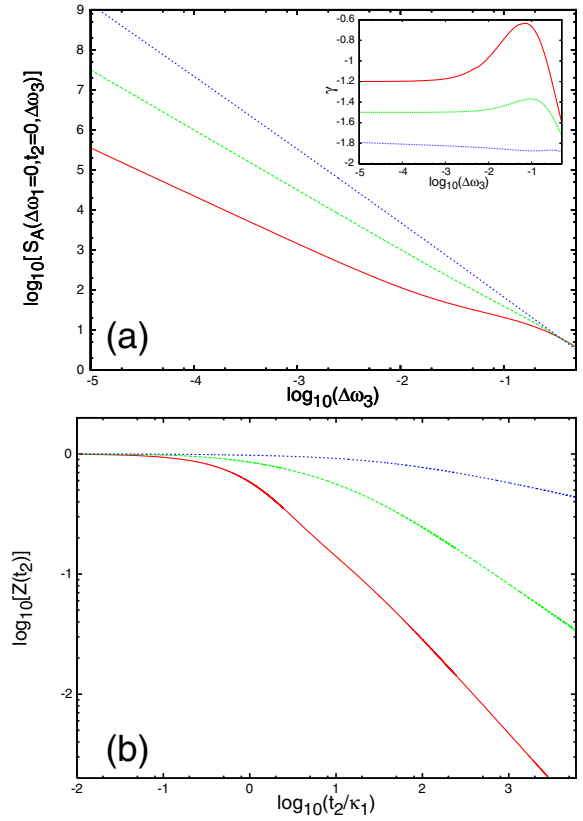

FIG. 2 (color online). Panel (a): Peak divergence along $\Delta\omega_1 = 0$. $t_2 = 0$, $\alpha = 1.2$ (dotted line), 1.5 (dashed line), and 1.8 (solid line). Other parameters are the same as in Fig. 1. Inset: peak exponent $\gamma \equiv \frac{d\log[S_A(\Delta\omega_1=0,t_2=0,\Delta\omega_3)]}{d\log[\Delta\omega_3]}$. Panel (b): $Z(t_2)$ for the WTDF [Eq. (6)] $\kappa_\alpha/\kappa_1 = 0.5$, $\Omega_0\kappa_1 = 1.0$, $\alpha = 1.2$ (dotted line), $\alpha = 1.5$ (dashed line), and $\alpha = 1.8$ (solid line), $\Omega_0 = 1$. Power-law growth of cross peaks is seen.

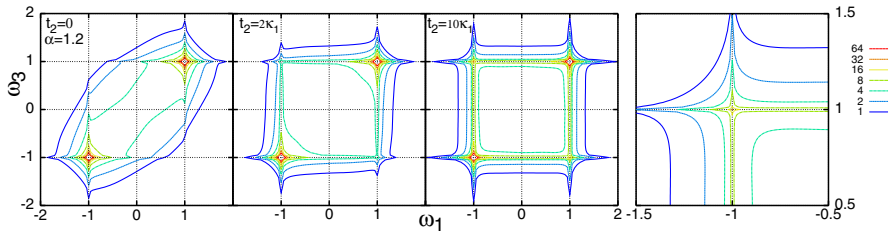

FIG. 3 (color online). Variation of the 2D S_A signal [Eq. (1)] for the WTDF [Eq. (6)] with the time delays (left to right) $t_2 = 0$, $2\kappa_1$, $10\kappa_1$. Other parameters same as Fig. 1(a). Right panel: Cross peak for $t_2 = 10\kappa_1$ on an expanded scale.

of the long-time memory, and S_A may not be factorized as in Eq. (4) at these frequencies. Outside these regions, or for finite Γ, the asymptotic line shape Eq. (4) is approached algebraically as t_2 is increased. By including a finite dephasing rate Γ, peak divergencies are cured and the line shapes resemble the normal relaxation case. However, the population evolution during t_2 is not affected by dephasing and the cross-peak dynamics is still anomalous. To study how the $(1, -1)$ cross peak grows to its long-time value [Eq. (4)], we have considered the quantity $Z(t_2) \equiv |S_A(\omega_1, t_2, \omega_3) - S_A(\omega_1, \infty, \omega_3)|/|S_A(\omega_1, 0, \omega_3) - S_A(\omega_1, \infty, \omega_3)|$ for $\omega_1 = 1$, $\omega_3 = -1$. Straight lines in log-log plots of $Z(t_2)$ vs t_2 [Fig. 2(b)] indicate algebraic relaxation. The asymptotic exponent [slope in Fig. 2(b)] approaches $\alpha - 1$, which is identical to that of the frequency correlation function $\langle \delta\Omega_{eg}(t)\delta\Omega_{eg}(0)\rangle$ [12].

Finally, we discuss aging effects which show up for $0 < \alpha < 1$, where κ_1 diverges. This describes nonergodic nonstationary processes which never equilibrate, and their properties change with time [19]. We model it by a random walk which is started by a jump at some fixed time. The response function depends on the time elapsed from the start of a random walk t_{in} to the first laser pulse at 0 [20,21]. This effect is fully described by allowing $\psi'(t; t_{in})$ to depend on t_{in}. In Laplace space, we find $\tilde{\psi}'(s; s_{in}) = [\tilde{\psi}(s_{in}) - \tilde{\psi}(s)]/[1 - \tilde{\psi}(s_{in})](s - s_{in})$ [22]. The nonlinear line shapes measured in the time-domain provide a direct measure of the response function, unlike frequency-domain measurements which involve stationarity in order to connect with response function [15]. However, due to the lack of equilibration, averaging over consecutive pulse sequences may depend on the repetition rate: A fresh ensemble with the same $\psi'(t)$ must be prepared before each application of the pulse sequence for the response function to be physically meaningful.

We have calculated the response functions for the model $\tilde{\psi}_N(s) = 1/[1 + (\kappa s)^\alpha]$, where $\psi(t) \sim (\kappa/t)^{1+\alpha}$ and $0 < \alpha < 1$. In Fig. 1(b), the S_A line shape is shown for $t_{in} = 0$; i.e., the random walk is started each time the first pulse interacts with the sample and $\psi'(t) = \psi(t)$ [19]. Microscopic reversibility breaks down for nonstationary processes, and obviously the symmetry [Eq. (3)] is violated. The nonstationary anomalous ensembles starts with some jump rate which depends on the initial preparation. At long times, it approaches the equilibrium value $1/\kappa_1$, which vanishes for the present model [21]. The higher rate during the (earlier) t_1 interval compared to t_3 results in broader peaks along ω_1 axis (compared to ω_3). Contour elongation along the $\omega_{1,3} = \pm 1$ axes is again observed with divergent diagonal peaks of complex structure. Our simulations demonstrate that two-dimensional correlation plots of the signals obtained from the response of the system to sequences of multiple laser pulses carry specific and direct signatures of complex dynamics.

The support of the MŠMT ČR (No. MSM 0021620835), NSF (No. CHE-0446555), and NIH (No. 2RO1GM59230-05) is gratefully acknowledged.

*Electronic mail: sanda@karlov.mff.cuni.cz
†Electronic mail: smukamel@uci.edu

[1] H. Frauenfelder, S. G. Sligar, and P. G. Wolynes, Science **254**, 1598 (1991).
[2] R. Metzler and J. Klafter, J. Phys. A **37**, R161 (2004).
[3] S. C. Kou and X. S. Xie, Phys. Rev. Lett. **93**, 180603 (2004).
[4] F. Amblard *et al.*, Phys. Rev. Lett. **77**, 4470 (1996).
[5] R. Verberk and M. Orrit, J. Chem. Phys. **119**, 2214 (2003).
[6] M. Kuno *et al.*, Phys. Rev. B **67**, 125304 (2003).
[7] K. T. Shimizu *et al.*, Phys. Rev. B **63**, 205316 (2001).
[8] S. Mukamel, Annu. Rev. Phys. Chem. **51**, 691 (2000).
[9] J. Wang, J. Chen, and R. M. Hochstrasser, J. Phys. Chem. B **110**, 7545 (2006).
[10] J. Zheng *et al.*, Science **309**, 1338 (2005).
[11] T. Brixner *et al.*, Nature (London) **434**, 625 (2005).
[12] F. Šanda and S. Mukamel, Phys. Rev. E **73**, 011103 (2006).
[13] M. F. Shlesinger, J. Stat. Phys. **10**, 421 (1974).
[14] X. Brokmann *et al.*, Phys. Rev. Lett. **90**, 120601 (2003).
[15] Y. Jung, E. Barkai, and R. Silbey, Chem. Phys. **284**, 181 (2002).
[16] S. Mukamel, *Principles of Nonlinear Optical Spectroscopy* (Oxford Univ. Press, New York, 1995).
[17] M. Khalil, N. Demirdöven, and A. Tokmakoff, Phys. Rev. Lett. **90**, 047401 (2003).
[18] Y. Tanimura, J. Phys. Soc. Jpn. **75**, 082001 (2006).
[19] J. Klafter, M. F. Shlesinger, and G. Zumofen, Phys. Today **49**, No. 2, 33 (1996).
[20] G. Aquino, L. Palatella, and P. Grigolini, Phys. Rev. Lett. **93**, 050601 (2004).
[21] F. Barbi, M. Bologna, and P. Grigolini, Phys. Rev. Lett. **95**, 220601 (2005).
[22] The long t_{in} limit (i.e., $s_{in} \to 0$) for CTRW with finite κ_1, reproduce the WTDF of the first jump of stationary random walk $\psi'(t; t_{in}) = \phi(t)/\kappa_1$.